

Fault Detection for Shipboard Monitoring – Volterra Kernel and Hammerstein Model Approaches

Zoran Lajic^{*}, Mogens Blanke^{**},^{***} and Ulrik Dam Nielsen^{*}

^{*} Technical University of Denmark, Department of Mechanical Engineering, Section of Coastal, Maritime and Structural Eng.
Build. 403, 2800-Kgs. Lyngby, Denmark {zl@mek.dtu.dk}, {udn@mek.dtu.dk}

^{**} Technical University of Denmark, Department of Electrical Engineering, Automation and Control Group
Build. 326, 2800-Kgs. Lyngby, Denmark {mb@elektro.dtu.dk}

^{***} Norwegian University of Technology and Science, Centre for Ships and Ocean Structures
7491 Trondheim, Norway

Abstract: In this paper nonlinear fault detection for in-service monitoring and decision support systems for ships will be presented. The ship is described as a nonlinear system, and the stochastic wave elevation and the associated ship responses are conveniently modelled in frequency domain. The transformation from time domain to frequency domain has been conducted by use of Volterra theory. The paper takes as an example fault detection of a containership on which a decision support system has been installed. Copyright © 2009 IFAC.

1. INTRODUCTION

The SeaSense system (Nielsen et al., 2006) has been installed on several containerships and navy vessels. The system provides an estimation of the actual sea state, information about the longitudinal hull-girder loading, sea-keeping performance of the ship, and decision support on how to operate the ship within acceptable limits. The system is able to identify critical forthcoming events and to give advice regarding speed and course changes to decrease the wave-induced loads. The SeaSense system sensors, sketched in Fig. 1, includes sensors, which are used to estimate hull stresses and predict wave loads, with the purpose of avoiding critical levels of hull stresses and ship motions. Detection of sensor faults is critical for the correct operation of the system. Several papers deal with maritime applications of fault-tolerant control systems. For example, a fault-tolerant sensor-fusion and control system for ship station keeping has been shown in (Blanke et al., 2005).

The present paper investigates possibilities to employ fault-diagnosis techniques to improve the dependability of the SeaSense system. Sensor fault diagnosis is considered using available measurements: vertical acceleration, heave, pitch, roll, wave elevation and relative wave height (distance between the deck and the water surface). The wave elevation could be obtained using the SeaSense system and it has been – artificially – included in the sensor fault detection procedure as a virtual sensor. The ship is a nonlinear system by nature. A linear model cannot be adopted for the ship sailing in heavy weather due to large roll angles and nonlinear vertical motions. Instead, a Volterra series approach is used to arrive at residuals for fault diagnosis. The Volterra theory is based on an approximation and the model is used to

investigate and justify a possible implementation of this theory. The results are compared with the residuals obtained by a Hammerstein model, which can be realized without any approximation. It is worth noting that is not always possible to use Hammerstein model(s). Hammerstein model(s) can be implemented only for systems, which have a particular separation between a static nonlinearity and a part with linear dynamics.

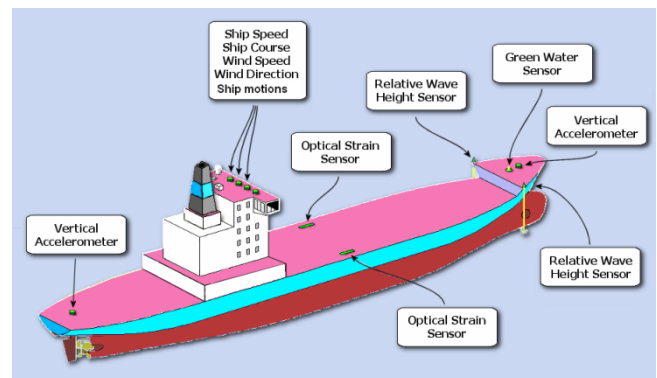


Fig.1: Onboard sensor arrangement

2. STRUCTURAL ANALYSIS

For the sensor fault detection, there is a need to find physical relations between measured values. The SeaSense system has at its disposal several measurements: vertical acceleration, heave, pitch, roll, wave elevation and relative wave height. In case sea state estimation is conducted by a ship-wave buoy analogy (e.g. Nielsen, 2006 and 2008), it is sufficient to use

three different ship motions (or responses). Therefore, the fault-tolerant approach is convenient for implementation in our case.

The relation between different ship motions are given by the following set of constraints:

$$c_1: z_b = z + \frac{L}{2} \sin \theta + \frac{B_b}{2} \sin \varphi, \quad (\theta \ll \varphi)$$

$$c_2: s_b = z_b - \zeta$$

$$d_1: \dot{z} = \frac{dz}{dt}, \quad d_2: \ddot{z} = \frac{d\dot{z}}{dt}, \quad d_3: \dot{z}_b = \frac{dz_b}{dt}, \quad d_4: \ddot{z}_b = \frac{d\dot{z}_b}{dt}$$

$$d_5: \dot{\theta} = \frac{d\theta}{dt}, \quad d_6: \ddot{\theta} = \frac{d\dot{\theta}}{dt}, \quad d_7: \dot{\varphi} = \frac{d\varphi}{dt}, \quad d_8: \ddot{\varphi} = \frac{d\dot{\varphi}}{dt}$$

$$m_1: y_1 = \dot{z}_b, \quad m_2: y_2 = z, \quad m_3: y_3 = \theta$$

$$m_4: y_4 = s_b, \quad m_5: y_5 = \zeta, \quad m_6: y_6 = \varphi$$

Where the variables are:

\ddot{z}_b	Vertical acceleration on the bow
z	Heave
θ	Pitch
φ	Roll
s_b	Relative bow motion (distance between the deck on the bow and the wave)
ζ	Wave elevation
L	Length of the ship
B_b	Breadth of bow section (on sensor position)

The longitudinal position of the accelerometer with respect to the centre of gravity is $L/2$ and vertical position is in the same level as the centre of gravity. For more information about constraints, see (Jensen, 2001).

The set of variables in the system is separated into the sets X (unknown) and K (known).

Known variables:

$$K = \{y_1, y_2, y_3, y_4, y_5, y_6\}$$

Unknown variables:

$$X = \{z_b, \dot{z}_b, \ddot{z}_b, z, \dot{z}, \ddot{z}, \theta, \dot{\theta}, \ddot{\theta}, s_b, \zeta, \varphi, \dot{\varphi}, \ddot{\varphi}\}$$

In order to extract the residuals, available for fault diagnosis, one may apply an analysis of the structure of the constraints and the unknown variables. While there are several ways to deduct analytical redundancy relations for nonlinear systems, structural analysis is particularly simple. Algorithms exist for matching unknown variables to constraints and find the non-matched constraints that are the basis for minimal structurally over-determined (MSO) sets that are used to determine the possible diagnosis algorithms (M. Krysander et al., 2008). Constraints are matched to the unknown variables as follows:

$$m_1(y_1) \rightarrow \dot{z}_b$$

$$m_2(y_2) \rightarrow z$$

$$m_3(y_3) \rightarrow \theta$$

$$m_4(y_4) \rightarrow s_b$$

$$m_5(y_5) \rightarrow \zeta$$

$$m_6(y_6) \rightarrow \varphi$$

$$c_1(z, \theta, \varphi) = c_1(m_2(y_2), m_3(y_3), m_6(y_6)) \rightarrow z_b$$

$$d_3(z_b) = d_3(c_1(m_2(y_2), m_3(y_3), m_6(y_6))) \rightarrow \dot{z}_b$$

$$d_1(z) = d_1(m_2(y_2)) \rightarrow \dot{z}$$

$$d_2(\dot{z}) = d_2(d_1(m_2(y_2))) \rightarrow \ddot{z}$$

$$d_5(\theta) = d_5(m_3(y_3)) \rightarrow \dot{\theta}$$

$$d_6(\dot{\theta}) = d_6(d_5(m_3(y_3))) \rightarrow \ddot{\theta}$$

$$d_7(\varphi) = d_7(m_6(y_6)) \rightarrow \dot{\varphi}$$

$$d_8(\dot{\varphi}) = d_8(d_7(m_6(y_6))) \rightarrow \ddot{\varphi}$$

Given a complete matching on the unknown variables, two constraints remain unmatched. Each of these gives basis for a residual generator that can check the consistency of the constraints. The residuals are:

$$r_1: d_4(z_b, \dot{z}_b) \rightarrow 0,$$

and after substitution of the unknown variables, obtained by backtracking through the matching (Blanke et al., 2006):

$$r_1: d_4(d_3(c_1(m_2(y_2), m_3(y_3), m_6(y_6))), m_1(y_1)) \rightarrow 0$$

$$r_2: c_2(z_b, s_b, \zeta) \rightarrow 0, \text{ or}$$

$$r_2: c_2(c_1(m_2(y_2), m_3(y_3), m_6(y_6)), m_4(y_4), m_5(y_5)) \rightarrow 0$$

The dependency matrix is shown in Table 1 where d denotes detectable and i a structurally isolable constraint.

As a result of the analysis, the following information about the variables can be obtained:

Detectable: $c_1, c_2, m_2, m_3, m_4, m_5, m_6$

Undetectable: none

Isolable: m_1

Table 1: Dependency matrix

/	c_1	c_2	m_1	m_2	m_3	m_4	m_5	m_6
r_1	1		1	1	1			1
r_2	1	1		1	1	1	1	1
	d	d	i	d	d	d	d	d

It should be noted that constraints d_1, d_2, \dots, d_8 are omitted from the dependency matrix, because these constraints are based upon the mathematical definition and they cannot fail. The residuals can be expressed in the analytic form as:

$$r_1 = y_1 - \ddot{y}_2 - \frac{L}{2} \frac{d^2}{dt^2} (\sin y_3) - \frac{B_b}{2} \frac{d^2}{dt^2} (\sin y_6)$$

$$r_2 = y_4 + y_5 - y_2 - \frac{L}{2} \sin y_3 - \frac{B_b}{2} \sin y_6$$

3. RESIDUAL TRANSFORM TO FREQUENCY DOMAIN

The residual r_1 is not implementable in the time domain due to derivatives. An appropriate filtering need be established. The filter design is straightforward in frequency domain. Therefore, the frequency domain model is needed. There are two alternatives for the present system:

- 1) Volterra expansion,
- 2) Representation of nonlinearities as a Hammerstein system.

3.1 Volterra Kernel Approach

Let us consider the first residual:

$$r_1: y_1 - \ddot{y}_2 - \frac{L}{2} \frac{d^2}{dt^2} (\sin y_3) - \frac{B_b}{2} \frac{d^2}{dt^2} (\sin y_6) = 0 \quad (1)$$

A first step is to develop $\sin y_3$ and $\sin y_6$ in the power series and to find second derivatives. In the following calculations only the first two members of power series will be used.

The residual must be transformed in a form convenient for implementing Volterra theory. Therefore, as a second step, r_1 must be rewritten in input/output form. The y_3 can be considered as an input and the output can be:

$$\ddot{y}_2 - y_1 + \frac{B_b}{2} (\ddot{y}_6 - y_6 \dot{y}_6^2 - \frac{1}{2} y_6^2 \ddot{y}_6) = u_3(t) \quad (2)$$

Now, the residual r_1 is of the following form:

$$-\frac{L}{2} \ddot{y}_3 + \frac{L}{2} y_3 \dot{y}_3^2 + \frac{L}{4} y_3^2 \ddot{y}_3 = u_3 \quad (3)$$

The basic idea is to divide the system in subsystems and to find Laplace transforms of these. The solution of Equation (3) can be written in the form (Rugh, 1981):

$$y_3(t) = \sum_m G_{m1, \dots, mN} (\lambda_1, \dots, \lambda_N) e^{(m1\lambda_1 + \dots + mN\lambda_N)t} \quad (4)$$

Then assume an input of the form (5) to find the first three symmetric transfer functions.

$$u_3(t) = e^{\lambda_1 t} + e^{\lambda_2 t} + e^{\lambda_3 t} \quad (5)$$

The system kernels in the frequency domain are transfer functions of the subsystems and have the following forms:

$$H_{1,3}(s) = G_{1,0, \dots, 0}(s) \quad (6)$$

$$H_{2,3sym}(s_1, s_2) = \frac{1}{2!} G_{1,1,0, \dots, 0}(s_1, s_2) \quad (7)$$

$$H_{N,3sym}(s_1, \dots, s_N) = \frac{1}{N!} G_{1, \dots, 1}(s_1, \dots, s_N) \quad (8)$$

Therefore $y_3(t)$ can be expressed using the expression:

$$y_3(t) = G_{100} e^{\lambda_1 t} + G_{010} e^{\lambda_2 t} + G_{001} e^{\lambda_3 t} + G_{200} e^{2\lambda_1 t} + G_{020} e^{2\lambda_2 t} + G_{002} e^{2\lambda_3 t} + G_{110} e^{(\lambda_1 + \lambda_2)t} + G_{101} e^{(\lambda_1 + \lambda_3)t} + G_{011} e^{(\lambda_2 + \lambda_3)t} + G_{111} e^{(\lambda_1 + \lambda_2 + \lambda_3)t} + \dots \quad (9)$$

Substituting (5) and (9) into equation (3) and equating the coefficients of:

$$e^{\lambda_1 t}, e^{(\lambda_1 + \lambda_2)t}, e^{(\lambda_1 + \lambda_2 + \lambda_3)t}$$

on the both sides of equation yields the equations:

$$-\frac{L}{2} G_{100} \lambda_1^2 = 1 \rightarrow G_{100}(\lambda_1) = \frac{-2}{L\lambda_1^2} \rightarrow H_{1,3}(s) = \frac{-2}{Ls^2} \quad (3.12)$$

$$-\frac{L}{2} G_{110}(\lambda_1 + \lambda_2)^2 = 0 \rightarrow H_{2,3sym}(s_1, s_2) = 0 \quad (10)$$

In the same way, noting that $G_{010} = \frac{-2}{L\lambda_2^2}$ and $G_{001} = \frac{-2}{L\lambda_3^2}$, $H_{3,3sym}$ -is:

$$H_{3,3sym}(s_1, s_2, s_3) = -\frac{4}{3L^3 s_1^2 s_2^2 s_3^2} \quad (11)$$

Transformation from $H_{3,3sym}(s_1, s_2, s_3)$ to $H_{3,3sym}(s)$ can be done using association of the 3rd order.

$$H_{3,3sym}(s) = A_3 [H_{3,3sym}(s_1, s_2, s_3)] \quad (12)$$

Association of Equation (12) gives the following solution (Rugh, 1981):

$$H_{3,3sym}(s) = -\frac{8}{L^3 s^4} \quad (13)$$

The transfer function is given by:

$$H_3(s) = H_{1,3}(s) + H_{3,3sym}(s) = -\frac{2L^2 s^2 + 8}{L^3 s^4} \quad (14)$$

$$Y_3(s) = H_3(s) U_3(s) \quad (15)$$

The next step is to find $U_3(s)$. The equation (2) can be written as:

$$\ddot{y}_2 - y_1 - u_3 = -\frac{B_b}{2} \ddot{y}_6 + \frac{B_b}{2} y_6 \dot{y}_6^2 + \frac{B_b}{4} y_6^2 \ddot{y}_6 \quad (16)$$

Equation (16) can be expressed in input/output form. With the input y_6 and output u_6 :

$$u_6 = \ddot{y}_2 - y_1 - u_3 \quad (17)$$

Or in the frequency domain:

$$u_6(s) = s^2 y_2(s) - y_1(s) - u_3(s) \quad (18)$$

The transfer function $H_6(s)$ can be found using the same procedure as in case of $H_3(s)$:

$$H_6(s) = -\frac{2B_b^2 s^2 + 8}{B_b^3 s^4} \quad (19)$$

Therefore:

$$Y_6(s) = H_6(s) U_6(s) \quad (20)$$

After inserting (18) and (19) in (20), it is easy to find U_3 .

$$u_3(s) = -\frac{B_b^3 s^4}{2B_b^2 s^2 + 8} y_6(s) + s^2 y_2(s) - y_1(s) \quad (21)$$

The residual r_1 in frequency domain can be obtained by inserting (14) and (21) in (15). So, the residual r_1 in frequency domain, after introducing the filter ($\alpha = 0.1$) is:

$$r_1(s) = \frac{\alpha^2}{(s+\alpha)^2} y_1(s) - \frac{\alpha^2 s^2}{(s+\alpha)^2} y_2(s) - \frac{L^3 \alpha^2 s^4}{(s+\alpha)^2 (2L^2 s^2 + 8)} y_3(s) - \frac{B_b^3 \alpha^2 s^4}{(s+\alpha)^2 (2B_b^2 s^2 + 8)} y_6(s) \quad (19)$$

In case of residual r_2 , it is possible to implement the same procedure which yields the result:

$$r_2(s) = \frac{\alpha}{s+\alpha} y_2(s) + \frac{\alpha L^3}{(s+\alpha)(2L^2+4)} y_3(s) - \frac{\alpha}{s+\alpha} y_4(s) - \frac{\alpha}{s+\alpha} y_5(s) + \frac{\alpha B_b^3}{(s+\alpha)(2B_b^2+4)} y_6(s) \quad (20)$$

3.2 Hammerstein Model Approach

A simple nonlinear system is the Hammerstein system. A Hammerstein system consists of a static nonlinear system followed by a linear dynamic system.

The transform to frequency domain is easy when the nonlinear system is a Hammerstein form. With the assumption of a Hammerstein system, residuals r_1 and r_2 can be transformed as shown in Fig. 2.

In the following, Simulink[®] simulations of the residuals r_1 and r_2 are presented.

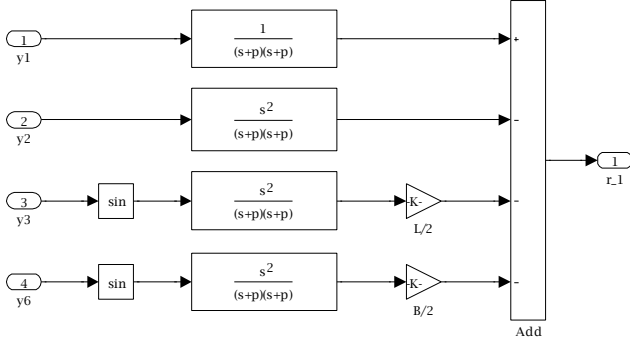


Fig. 2: Residual r_1 in frequency domain (Hammerstein system) – Simulink model.

The applied models are given in the frequency domain and transformed using Volterra series or using the Hammerstein model representation. The simulation of ship motions in waves is similar to (Nielsen, 2007). The ship considered is a containership (length $L=275$ m, breadth $B=40$ m, draught $T=12$ m), which sails at speed of 10 m/s. The wave elevation is shown in Fig. 3 and simulated ship responses are shown in Fig. 4.

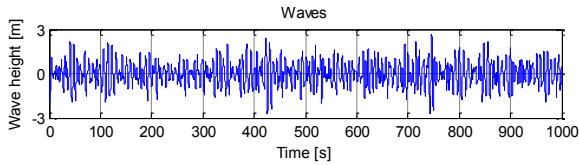


Fig. 3: Wave elevation (midship section)

Residual r_1 in case of no faults for Hammerstein model and the agreement with Volterra model are shown in Figure 5. Figure 6 shows the residual r_2 . There is extremely good agreement between the two models.

4. RESIDUAL EVALUATION AND SIMULATION TESTS

In the following, the residuals in the presence of faults will be shown and discussed. As examples of fault scenarios, the faults will be created by adding an extra signal to the sensor output during time interval between 100 and 500 s. After 500 s, faults are removed. Faults are simplified to occur as stepwise signals. The scenario is detailed in Table 2. where: f_1 - fault on vertical acceleration sensor, f_2 - fault on heave sensor, f_3 - fault on pitch sensor, f_4 - fault on wave elevation

sensor, f_5 - fault on relative wave height sensor and f_6 - fault on roll sensor.

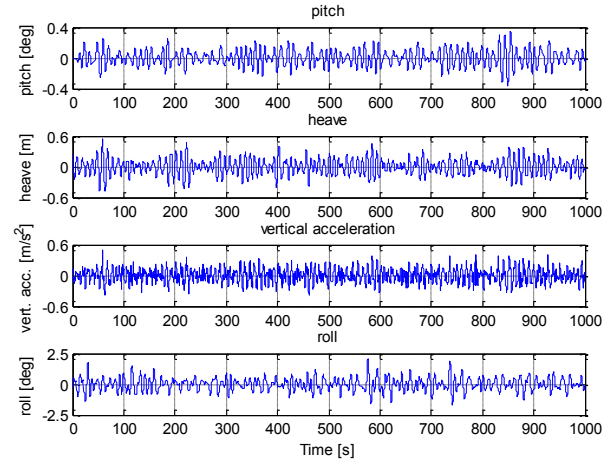


Fig. 4: Ship responses on the waves

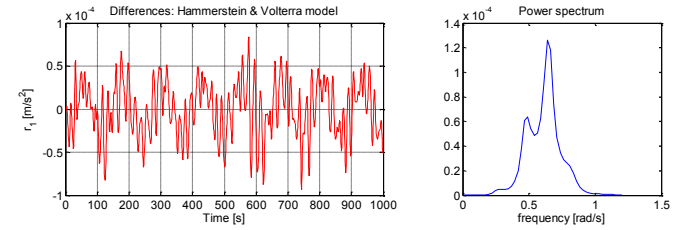
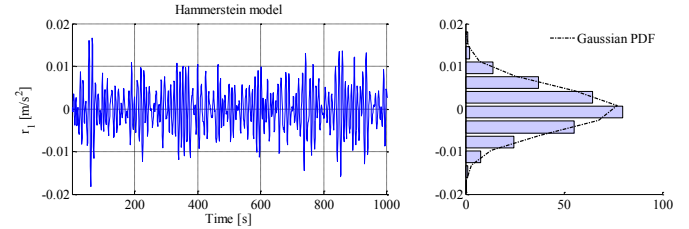


Fig. 5: Residual r_1 (no faults) amplitude distribution – frequency spectrum of r_1 and difference between Hammerstein and Volterra models.

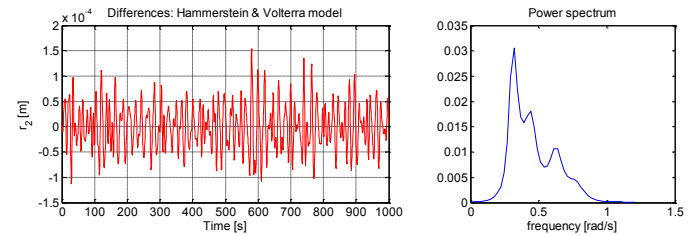
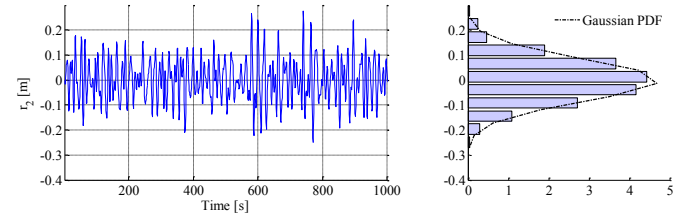


Fig 6. Residual r_2 (no faults), amplitude distribution – frequency spectrum of r_2 and difference between Hammerstein and Volterra models.

Table 2: Simulated faults.

Fault	Type	Units	Value	Time [s]
f_1	vertical acceleration	m/s ²	0.01	100-500
f_2	heave	m	0.1	100-500
f_3	pitch	deg	0.1	100-500
f_4	wave elevation	m	0.1	100-500
f_5	relative wave height	m	0.1	100-500
f_6	roll	deg	0.2	100-500

The fault signatures are shown in Table 3. In the following table a fault presence in the residual is marked with a symbol s or w . The letter s denotes strong detectability and w weak detectability.

Table 3: Fault signatures

	f_1	f_2	f_3	f_4	f_5	f_6
r_1	s	w	w	0	0	w
r_2	0	s	s	s	s	s
	i	d	d	d	d	d

The symbol i denotes fault isolability and the d is detectability. All six column vectors are different from zero, and thus all faults are detectable. The fault f_1 has a unique signature (s & 0) and is isolable. Residuals r_1 and r_2 are the same for both Hammerstein and Volterra models. Therefore, we present just one diagram for the residual r_1 and one for the residual r_2 .

Figures 5 and 6 show histograms of the residuals, and their frequency spectra. Histograms confirm that they both have Gaussian distribution, the frequency spectra show that the bulk of energy is at wave frequencies, as one would expect in this application. With peaks in the range 0.3 – 0.7 rad/s, filtering to reduce covariance in the residuals becomes obvious.

4.1 Change detection

Residual evaluation is based on the log likelihood test, as usual in change detection literature (Basseville & Nikiforov, 1993). In this case the change from normal (θ_0) to not normal condition (θ_1), where θ_1 has unknown magnitude takes place at a hypothetical change time, j . The log-likelihood ratio considered is then (Blanke et.al, 2006, p249):

$$S_j^k(\theta_1) = \sum_{i=j}^k \frac{\ln(p(\theta_1|r(i)))}{\ln(p(\theta_0|r(i)))}$$

And the generalised likelihood ratio test function (GLR) takes the form:

$$g(k) = \max_{0 \leq j \leq k} \max_{\theta_1} S_j^k(\theta_1)$$

The GLR decision function is used in the sequel in three different forms. When a fault is strongly detectable, the GLR is used to detect an unknown change of mean value and the test function is, for a scalar residual with mean μ_0 before the fault and variance σ^2 before and after the fault:

$$g(k) = \frac{1}{\sigma^2} \max_{k-M < j \leq k} \frac{1}{k-j+1} \left(\sum_{i=j}^k (r(i) - \mu_0) \right)^2. \quad (21)$$

Where M is a window size chosen appropriately.

When a fault is weakly detectable, and appears at the hypothetical instant k_0 , the GLR is used in a form where a known vector profile, $\rho(i-j) \equiv \rho_{i-j}$, of unknown amplitude ν , is to be detected in a vector residual with covariance \mathbf{Q} and mean μ_0 in the no-fault case (Blanke et.al:2006, p 259). The maximum likelihood estimate of the magnitude is, at time k , assuming the fault appeared at time j :

$$\hat{\nu}_{kj} = \left(\sum_{i=j}^k \rho'_{i-j} \mathbf{Q}^{-1} \rho_{i-j} \right)^{-1} \sum_{i=j}^k \rho'_{i-j} \mathbf{Q}^{-1} (\mathbf{z}_i - \mu_0),$$

and the decision function is

$$g(k) = \max_{k-M < j \leq k} \left\{ \hat{\nu}_{kj} \sum_{i=j}^k \rho'_{i-j} \mathbf{Q}^{-1} (\mathbf{z}_i - \mu_0) - \frac{\hat{\nu}_{kj}^2}{2} \sum_{i=j}^k \rho'_{i-j} \mathbf{Q}^{-1} \rho_{i-j} \right\}$$

(22)

This GLR decision function is used below to detect a profile in the residual. The profiles are determined from Eq. (19) and (20), taking the inverse Laplace transforms of the relevant operators, filter functions multiplied by Laplace operator of fault.

4.2 Results

The residuals were evaluated by the scalar GLR test, Eq. 21, using the same horizon $M=50$.

In case of the fault f_3 it was possible to use both residuals, but better results are obtained using the second residual. The residual r_1 in case of the fault f_3 has weak detectability and the detection of the dynamic profile is not possible for such low magnitudes of the fault. Therefore, the GLR with known dynamical profile of the fault Eq. (22) was implemented, but significant improvement wasn't obtained, again because it is the r_2 part that dominate in the detection when the covariance on r_1 is dominating. The residuals in the presence of a fault f_3 and the results of the GLR tests are shown in Fig. 8 and a histogram of residual r_2 in Fig. 9. The alarm diagram is constructed using a decision function and an appropriate threshold. Figure 9 compares the histograms of a residual in normal and faulty cases for a fault that is strongly detectable in the residual. The difference in probability distribution functions confirm that a mean value change detector could be

used. The residuals in the presence of fault f_6 are shown in Fig. 9 and vector case in Fig. 10.

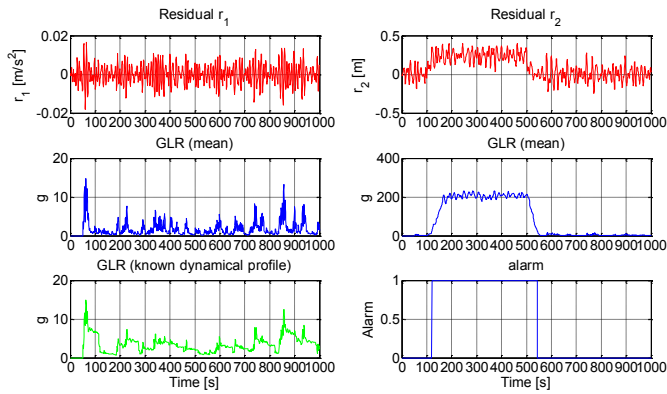


Fig. 7: Residuals r_1 & r_2 , fault $f_3 = 0.1$ deg, $\forall t \in [100 \text{ s}, 500 \text{ s}]$

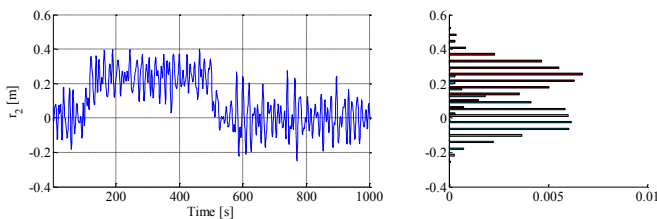


Fig. 8: Residual r_2 , fault $f_3 = 0.1$ deg, histogram.

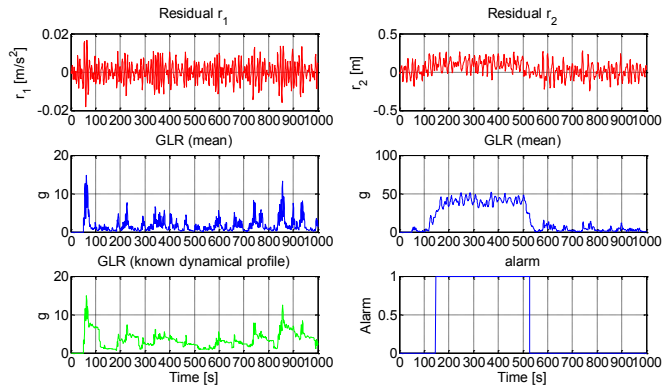


Fig. 9: The first row shows residuals r_1 & r_2 , with fault $f_6 = 0.2$ deg, $\forall t \in [100 \text{ s}, 500 \text{ s}]$. The second row shows $g(k)$ for scalar change detectors, the lowest row shows $g(k)$ for known dynamical profile of the fault in case of r_1 and alarm in case of r_2 .

5. CONCLUSIONS

In this paper, onboard sensor fault detection for monitoring and decision support systems has been presented. The ship is modelled as a nonlinear system, and therefore, the possibility of using the Volterra method to transform the nonlinear system from time domain into frequency domain was investigated. The faults were created by adding an extra signal to the sensor's output and the sensitivity of the residuals to the sensor fault was investigated. The residuals were evaluated by the GLR test, and all the faults were detected. The results were compared with a Hammerstein model and perfect agreement was obtained. Therefore the

implementation of the Volterra method has been justified and could be used in cases where nonlinearities could not be represented in Hammerstein form.

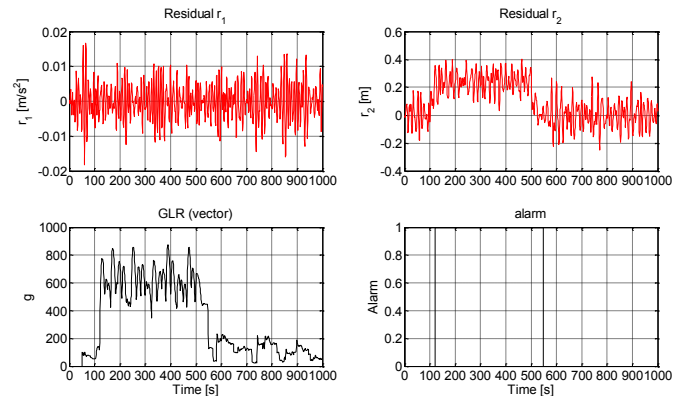


Fig. 10: Vector case, fault $f_3 = 0.1$ deg, $\forall t \in [100 \text{ s}, 500 \text{ s}]$, fault profile from r_1 detected in r_2 .

6. ACKNOWLEDGMENTS

The inspiring discussions with Professor Jørgen Juncher Jensen during the writing of this paper are highly appreciated. The present work has been supported by Danish Centre of Maritime Technology (DCMT).

7. REFERENCES

- Basseville, M. and I. Nikiforov (1993): *Detection of Abrupt Changes: Theory and Application*. Prentice-Hall.
- Blanke, M. (2005). Diagnosis and fault-tolerant control for ship station keeping, *Proc. 13th Mediterranean Conference on Control and Automation*, Limassol, Cyprus.
- Blanke, M., M. Kinnaert, J. Lunze, M. Staroswiecki (2006). *Diagnosis and Fault Tolerant Control*, Springer - Verlag, Berlin Heidelberg.
- Jensen, J.J. (2001). *Load and Global Response of Ships*, Elsevier, Oxford.
- Krysanter, M., J. Ålsund and M. Nyberg (2008). An efficient algorithm for finding minimal over-constrained subsystems for model-based diagnosis. *IEEE trans. on Systems, Man and Cybernetics - Part A: Systems and Humans*, 38(1).
- Nielsen, U.D. (2006). Estimations of on-site directional wave spectra from measured ship responses, *Marine Structures*, Vol. 19, pp. 33-60.
- Nielsen, U.D (2007). Response-based estimation of sea state parameters- influence of filtering, *Ocean Engineering*, Vol.34, Issue.13, 1797-1810.
- Nielsen, U.D. (2008), Introducing two hyperparameters in Bayesian estimation of wave spectra, *Probabilistic Engineering Mechanics*, Vol. 23, pp. 84-94.
- Nielsen, J.K., N.H. Pedersen, J. Michelesen, U.D. Nielsen, J. Baatrup, J.J. Jensen, E.S. Petersen(2006). SeaSense – Real-time Onboard Decision Support, *Proceedings of WMTC2006*, London, UK.
- Rugh, W.J (1981). *Nonlinear System Theory*, The Johns Hopkins University Press, Baltimore.